Graphene Oxide a New Carrier for Slow Release of Plant Micronutrients

*Shervin Kabiri[†], Fien Degryse [§], Diana N.H. Tran[†], Rodrigo C. da Silva [§], Mike J. McLaughlin *[§] and Dusan Losic*[†]*

[†]School of Chemical Engineering, Engineering North Building, The University of Adelaide, Adelaide, SA 5005, Australia

[§]Fertilizer Technology Research Centre, School of Agriculture, Food and Wine, The University of Adelaide, Waite Campus, PMB1, Glen Osmond, SA 5064, Australia

ABSTRACT: The environmental problems and low efficiency associated with conventional fertilizers provides an impetus to develop advanced fertilizers with slower release and better performances. Here we report of development of a new carrier platform based on graphene oxide (GO) sheets that can provide a high loading of plant micronutrients with controllable slow release. To prove this concept two micronutrients zinc (Zn) and copper (Cu) were used to load on GO sheets and hence formulate GO-based micronutrients fertilizer. The chemical composition and successful loading of both nutrients on GO sheets were confirmed by X-ray photoelectron spectroscopy (XPS), thermal gravimetric analysis (TGA) and X-ray diffraction (XRD). The prepared Zn-graphene oxide (Zn-GO) and Cu-graphene oxide (Cu-GO) fertilizers showed a biphasic dissolution behaviour compared to commercial zinc sulphate and copper sulphate fertilizer granules, displaying desirable fast- and slow-release micronutrient release. A visualization method and chemical analysis were used to assess the release and diffusion of Cu and Zn in soil from GO-based fertilizers compared with commercial soluble fertilizers to demonstrate the advantages of GO carriers and show their capability to be used as generic platform for macro- and micro-nutrients delivery. A pot trial demonstrated that Zn and Cu uptake by wheat was higher when using GO-based fertilizers compared to standard zinc or copper salts. This is a first report on the agronomic performance of GO-based slow-release fertilizer.

Key words: graphene oxide, micronutrients, slow release, fertilizers, carrier.

INTRODUCTION

Plant micronutrients are only needed in small amounts, but are essential for the growth and development of crops. Therefore, micronutrient fertilizers have been applied for many years to optimize plant yield.[1] Among the essential trace elements, zinc (Zn) plays a critical role in maintaining healthy root systems, in activating enzymes and detoxifying free radicals, and in preserving tolerance to plant stressors.[2] Zinc deficiency not only affects crop growth, but also is critical for human health. Zinc deficiency is the fifth leading risk factor for illness and death of children in developing countries where grain is an essential component of their staple diets.[3] Copper (Cu) is also considered as one of the essential trace elements for plant growth and development. It has vital roles in the metabolism of plants and controlling fungal

disease.[4] Although the plant's demand for Cu is relatively low compared to most other micronutrients, the consequence of Cu deficiency is still devastating to plants and may result in poor crop yields affecting food supplies.[5]

Most of the conventional micronutrients applied as fertilizers globally are water-soluble salts that include mainly sulphates or their chelated forms. In acidic sandy soils and high rainfall environments soluble and chelated micronutrients may be lost by leaching and run-off, which leads to high dosage requirements, serious environmental problems and economic costs.[6, 7] Another limiting factor is the strong retention of micronutrients in soil, either through strong adsorption reactions to clays and organic matter, or precipitation of insoluble compounds in the soil that dramatically reduce the efficacy of micronutrient fertilizers. One method that has been considered as a solution for these problems involves the use of slow-(SRFs) or controlled-release fertilizers (CRFs) which provide plant essential nutrients in a slower mode compare to traditional fertilizers. CRFs may play an important role in increasing crop efficiency due to sustained correction of mineral deficiency, and reductions in the frequency of fertilization, thereby minimising costs and reducing environmental pollution.[8] Therefore, development of CRF technologies to control the release of nutrients from soluble fertilizers has attracted tremendous attention in last two decades.[9] Currently most research on CRF technologies is directed to regulating nitrogen (N) release from fertilizers. Very few types of controlled release micronutrient fertilizers are commercially available, and they are generally based on insoluble oxides and their mixture with polyphosphates.[10] This concept using a short-chain polyphosphate has been explored for the slow release of Cu and Zn based micronutrients fertilizers.[6, 11, 12] Although these formulations have suitable properties for SRFs, their major drawback is the very high cost hence making them unprofitable for broad acre farming.[13, 14] The release mechanisms of the nutrients from these CRFs are based on either diffusion through their coating or slow hydrolysis. However, soil parameters such as water content, pH, ionic content and temperature are other factors that affect nutrient release by hydrolysis or diffusion. Therefore, there is a potential mismatch between the release rates of the micronutrients to the soil and the required rate of nutrient uptake by crops.[7, 15]

In the past few years, graphene has attracted enormous research interests due to its unique 2-d structure, high surface area and remarkable structural, mechanical, thermal, optical and electrical properties desired for many applications.[16-19] One of the most common approaches to graphene-based materials is to use of graphene oxide (GO) because of its scalable and low cost production from graphite.[20] Graphene oxide is a water-dispersible derivative of graphene showing high density of oxygen functional groups (carboxyl, hydroxyl, carbonyl and epoxy) in the carbon lattice and is produced by chemical oxidation of graphite.[21] The presence of different oxygen functional groups on the surface and edges of GO sheets makes it a unique and easily accessible substrate for multivalent functionalization and efficient loading of molecules.[22] Since 2008, after the first report by Dai et al.[23] showing the use of GO as an efficient nanocarrier for drug delivery, enormous number of studies have

been carried out to explore and apply GO carriers for wide spread biomedical applications ranging from drug/gene delivery, plant biology, biological sensing and imaging to biocompatible scaffold for cell culture.[24-28] The exciting achievements obtained on biomedical applications of graphene make these materials very attractive for nutrient delivery in agriculture and development of a novel class of slow-release fertilisers.

Beyond the biomedical application of graphene-based materials, a variety of studies have described the applications of these materials for the removal of inorganic species from aquatic environments.[20, 29] Most of these studies have employed GO as adsorbent for the removal of metal ions from water due to GO's high content of oxygen functional groups available for interaction with metal ions. Furthermore, the high specific surface area (theoretical 2620 m^2/g) of graphene-based materials make them an ideal candidature for processes involving adsorption or surface reactions.[30 31] The adsorption capacity of Cu^{+2} by GO (46 mg Cu g^{-1}) is around 10 times more than activated carbon.[32] The adsorptive property of GO was investigated for Cu^{+2}, Zn^{+2}, Cd^{+2} and Pb^{+2} where the following maximum sorption capacities were observed: 294, 354, 530 and 1119 mg g^{-1}, respectively.[33 34-36] Considering the high adsorption capacity of GO for metal ions and its application as carrier for loading and delivery of therapeutic molecules, it is reasonable to expect that GO could be successfully used as carrier for plant micronutrients.

Several studies have investigated the short- and long-term impact of graphene-based materials in animal or cell modules, plant and on the environment.[24, 28, 37-40]These studies show that there are several factors influencing the interaction of graphene-based materials with biological cells, including the lateral size, surface structure, functionalization, charge, impurities, aggregations, and corona effects.[41-43] Based on these studies by increasing the hydrophilicity or dispensability of graphene-based materials their biocompatibility will increase.[44] Therefore, GO sheets with large numbers of hydrophilic groups on their surface and edges are more likely to be biocompatible with animal and plant cells.[24] Furthermore, different studies have highlighted the significance of an eco-friendly enzymatic degradation strategy using peroxidase family of enzymes, such as horseradish peroxidases, myeloperoxidases and lignin peroxidase (a ligninolytic enzyme released from white rot fungus) to degrade graphene-based materials.[45-47] Therefore, GO could be degraded efficiently on the soil due to the presence of huge amount of white rot fungi or lignin peroxidase, in nature and avoid environmental pollution.

Currently used micronutrient fertilizers generally have fast release, which may cause considerable loss of nutrients, thus lowering their efficiency and increasing the cost of the crop production. In this work, we present a new concept to address these limitations and demonstrate the use of GO sheets as new carriers for large capacity loading of plant micronutrients and their application for advanced fertilizers with sustained and slow release. The idea is based on the unique properties of GO, having an ultra large surface area and high density of oxygen functional groups on the surface that can provide

electrostatic interaction and affinity for binding and loading of metal ions used as micronutrients. Figure 1 shows the scheme of proposed concept showing loading and release of Cu and Zn ions on GO sheets and preparation of Cu-GO and Zn-GO solid fertilizer in the form of pellets. Here, we explored the performance of these new graphene-based micronutrient fertilizers by evaluating their loading capacity and release performance in solution and soil and their availability to plants.

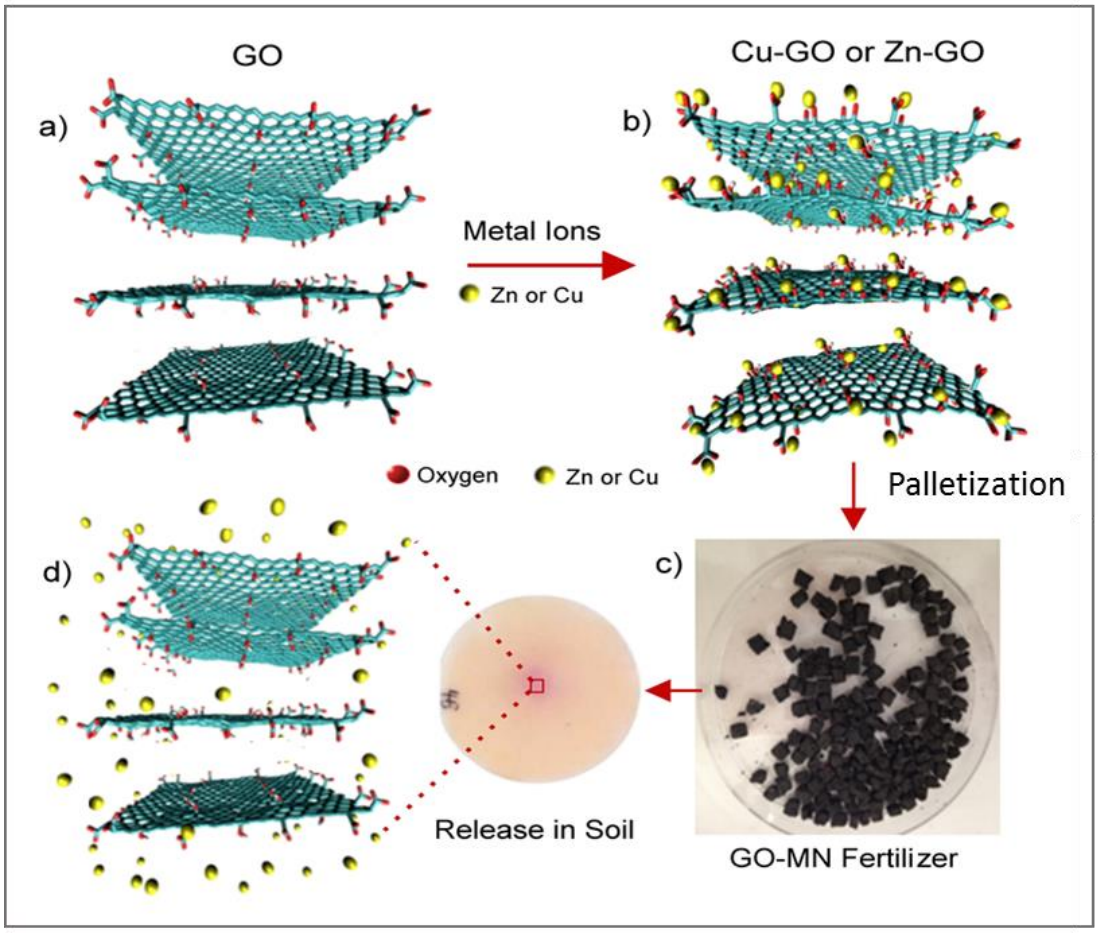

Figure 1. A schematic of the preparation and release of slow release micronutrients graphene oxide-zinc/copper based fertilizers. (a) GO prepared from natural graphite rocks by the acid exfoliation process with different functional groups (-OH and –COOH) used as micronutrients carrier, (b) GO sheets loading with micronutrients, Cu or Zn metal ions attached to the oxygen functional groups on the surface and edges of the sheets, (c) Photos of the prepared GO-micronutrients (GO-MN) fertilizer in form of the pellets (Cu-GO or Zn-GO), and (d) the release study in soil using prepared pellets (Cu-GO or Zn-GO) showing slow release of micronutrients from GO carriers.

RESULTS AND DISCUSSION

The SEM and TEM image of GO used as micronutrients carrier, confirming their typical size, irregular shape and few layers thickness (Figure 2 a-b). Their thickness was more precisely determined by AFM showing presence of oxidized functional groups on surface of single GO sheet (Figure 2c).[48, 49] Further characterization carried out using X-ray diffraction spectroscopy (XRD, Figure 2d) showed a major peak 2θ peak graphite at 26.6° that corresponding to an

interplanar spacing of (002) hexagonal layers of carbon atoms. This intensive peak disappears in the XRD pattern of GO sheets and is replaced with a broad and weak peak at 2θ = 9.9° that is characteristic of GO.[50] Fourier transform infrared spectroscopy (FTIR) and X-ray photoelectron spectroscopy (XPS) confirmed the presence of oxygen-containing functional groups on the surface of GO which have been discussed in detail in the Supporting Information (Figure S1).

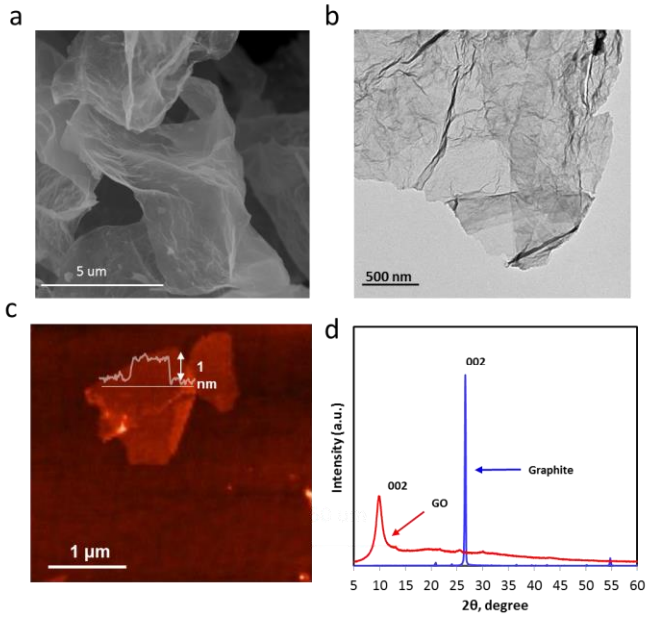

Figure 2. Characterization of graphene oxide (GO) used as micronutrients carrier: (a) SEM and (b) TEM, (c) AFM images of single GO sheets confirming a few layers thickness; and (d) XRD pattern of graphite and graphene oxide (GO).

To confirm the capability of GO as a carrier for different micronutrients, a series of batch adsorption experiments were conducted in which the adsorption capacity of GO for Cu and Zn were determined. The influence of pH on the adsorption of these metal ions on GO surface was initially explored because pH affects the speciation of these metal ions, as well as the surface properties of the GO sheets. This is relevant for determining the adsorption capacity of Zn and Cu on GO sheets and to prevent the precipitation of their oxide or hydroxides. Figure 3a showed the adsorption of both Cu and Zn ions increased gradually from pH 3-6 and remained constant at pH 6-7 before decreasing at pH 8. At a low concentration of Cu within the pH range of 3-7.5, Cu^{+2} is the dominant species of Cu species, while copper hydroxide ($Cu(OH)_2$) is predicted to be the dominant species at higher pH values up to 12.3 (Supporting Information Figure S2).[51] Furthermore, the pH_{pzc} (point of zero charge) value of GO is 3.8-3.9, which means at pH values > 3.9, GO is negatively charged and thus the electrostatic interactions of the positively charged metal ions and the negative surface of the GO sheets becomes stronger.[33, 52] At higher pH the formation of hydroxide complexes of copper ($CuOH^+$) in solution occurs, hence the adsorption of Cu decreases due to the lower positive charge and electrostatic attraction of ($CuOH^+$) compare to Cu^{+2}.[31, 51] In the case of Zn, the adsorption more sharply increases with pH from pH

3 to 6, as the predominant Zn species is Zn^{+2} in the pH range of 3-6 and the increasing negative charge on the GO sheets with increasing pH thus results in stronger adsorption. The low adsorption of Zn^{+2} on the GO sheets at pH 3 could be due to the competition between H^{+} and Zn^{+2} for the same sorption sites.[31] The slight decrease of Zn adsorption at pH 7-8 can be explained by the formation of $Zn(OH)_2$ that are precipitating in the solution. Furthermore, at high pH values, the predominant Zn specious is $Zn(OH)^{-}_3$, which is difficult to be adsorbed on negatively charged GO.[31]These results for Zn and Cu adsorption on GO are in agreement by previous studies reported in literature performed for different reasons (water purifications).[30, 31]

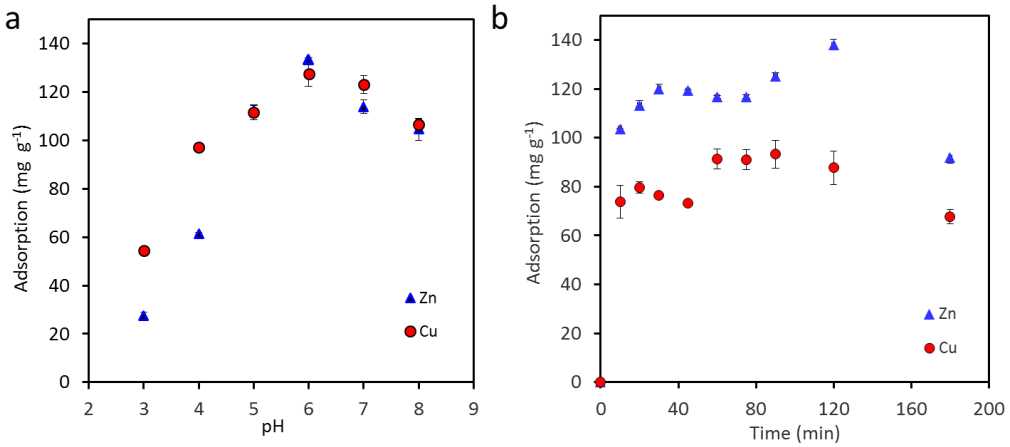

Figure 3. a) Influence of pH on adsorption of Zn and Cu (20 mg L^{-1}) on GO sheets (5 mg) and (b) kinetic study of Zn and Cu adsorption at pH of 6 and 4.5 for Zn and Cu adsorption, respectively (with initial concentration of 20 mg L^{-1} for both Zn and Cu).

The kinetic rate of adsorption for these two metal ions on the GO sheets using optimised pH conditions (pH 6) was determined and is presented in Figure 3b.[53] The results show a significant increase in adsorption of both ions at the beginning of the process (first 10 minutes) with slow increase after 10-20 minutes and reaching maximum after 120 min. The amount of solute adsorbed per gram GO (q_e) determined from the experimental data was 137 mg g^{-1} and 93 mg g^{-1} for Zn^{+2} and Cu^{+2}, respectively. Both pseudo-first and pseudo-second-rate adsorption kinetic models were used to study the kinetics of the sorption process (Supporting Information S3). [34, 53] The experimental values q_e were close to the calculated q_e values from the pseudo-second-order equation (133 mg g^{-1} and 73 mg g^{-1} for Zn^{+2} and Cu^{+2}, respectively). The presented pseudo-second-order kinetic models also showed higher value of correlation coefficients (R^2 values) compared to the pseudo-first order models. This suggests that the sorption of Zn and Cu ions is controlled by chemical adsorption and strong attachment of those ions to the oxygen functional groups on the surface of the GO sheets (Supporting Information Table S3).[31] The conclusion can be made that the adsorption capacity of the GO is directly related to the number of active sites that exist on the GO surface.[31, 32]

To gain insight into the chemical composition of the prepared GO-based micronutrients and to investigate the nature of the chemical binding between the metal ions and GO sheets, XPS

characterizations were performed. Selected survey and high-resolution graphs for specific elements obtained from GO sheets before and after Zn and Cu ions adsorption are presented in Figure 4 and (Supporting Information, S4). The appearance of Zn (Zn 3s/3p) and Cu (Cu 3s) peaks in the survey spectra of Zn-GO and Cu-GO, respectively, confirm the presence of the metal ions (Zn 4.34 %, Cu 6.2%) on the GO structures (Supporting Information, Table S4). High resolution analysis of C1s and O1s for both Zn-GO and Cu-GO composites are presented in Figure 4a and b. Deconvolution of the C1s spectrum for GO showed that the primary peak at 285 eV can be attributed to the sp^2-hybridized carbon of the GO sheets (Figure 4a). The peak was asymmetric due to the presence of other carbon functionalities including sp^3/aliphatic hydrocarbon species and carbon–oxygen species such as C–OH, C–O–C, C=O, and C–OOH.[49] The C1s spectra of Zn-GO and Cu-GO composites is also fitted to four peaks corresponding to C=C or C-C, C-O, C=O and O=C-O. However, the binding energy of the C=O and O=C-O peaks of Zn-GO and Cu-GO composites were slightly shifted towards higher bonding energy directions after Zn and Cu binding, which indicates the inclusion of the metal ions on the GO matrix.[31, 54, 55] Furthermore, the O1s XPS spectra of GO, Zn-GO and Cu-GO and the binding energies of oxygen in the various functional groups were allocated according to those in the literature (Figure 4b).[49, 56] The O1s spectrum of GO without metal ions is significantly different both in position, shape and maximum intensity from the spectra for GO with adsorbed Zn and Cu ions. This result confirms the involvement of the oxygen functional groups presented on the surface of GO on the sorption of the metal ions, that is in agreement with previous studies.[31, 55]

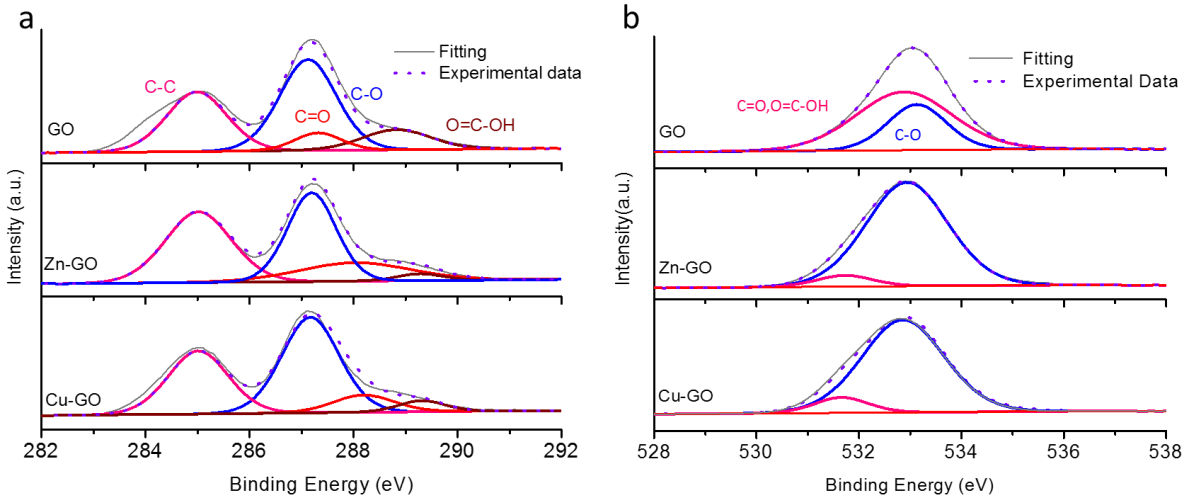

Figure 4. The high-resolution XPS spectra of (a) C1s and (b) O1s obtained from GO sheets before and after metal ion adsorption (Zn-GO and Cu-GO).

Further characterisation to confirm the attachment of metal ions on the GO surface was performed using Raman, XRD and TGA characterizations. The Raman spectrum of GO (Figure 5a) showed the characteristic D and G bands at 1341 and 1595 cm^{-1}, respectively. The Raman plots of Zn-GO and Cu-GO also contained both the G and D bands, but the occurrence of a mild

blue shift of the 'G band' (~9 cm^{-1}) for both Zn-GO and Cu-GO, and a red shift of the 'D band' (~8 cm^{-1}) for Cu-GO composites suggested that the Zn and Cu functionalization altered the structural vibrations of the Zn-GO and Cu-GO composites.[55]

The X-ray diffraction pattern of GO showed a predominate peaks at $2\theta \sim 9.86°$ (Figure 5b), which can be assigned as the (001) reflection corresponding to the graphite interlayer distance. This (001) reflection was also observed for the Cu-GO and Zn-GO composites. However, this peak shifted to lower 2θ values (ca. 9.08º and 9.64º for Cu-GO and Zn-GO, respectively), which is evidence of the intercalation of the metal ions.[54] Furthermore, a significant peak broadening was observed for Cu-GO and Zn-GO compared to GO, that may originate from the particle (crystallite) size broadening or lattice strain broadening.[57] No diffraction peaks from any other impurities (such as metal oxides) were detected in the XRD data of Cu-GO and Zn-GO.

The comparative thermogravimetric (TGA) graphs of the GO, Zn-GO and Cu-GO loaded GO carriers performed by a (TG) analyser are presented in Figure 5c. GO is thermally unstable and starts to lose mass upon heating even below 100 ºC. The major weight loss (~70%) occurs at ~300 °C, which is probably due to the pyrolysis of the liable oxygen-containing functional groups.[58] Although both Zn-GO and Cu-GO followed a similar profile as GO, their thermal stability increased compared to GO. The TG curve of GO showed a weight loss of ~98%, while the TG curves of Zn-GO and Cu-GO shoed lower weight losses (~86-90%) compared to bare GO, confirming the presence of Zn and Cu in the GO structure.

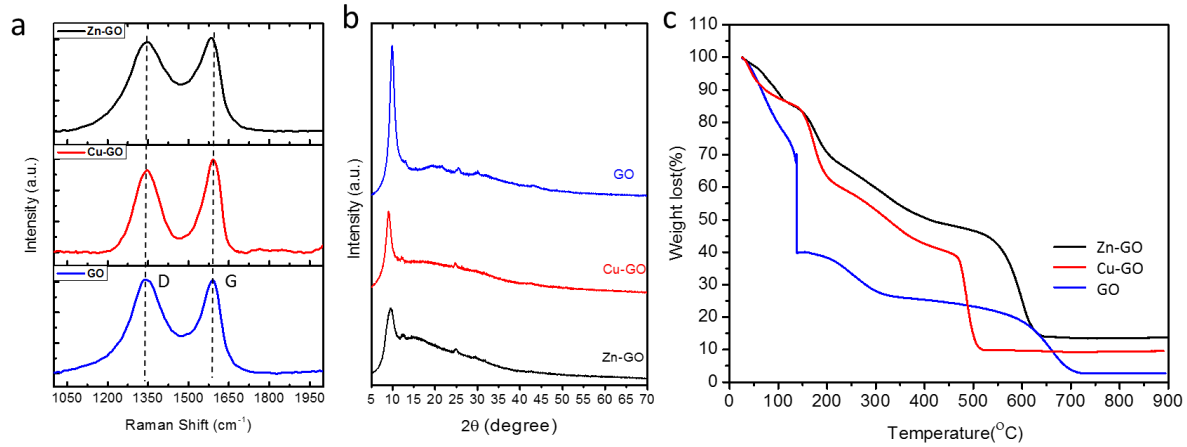

Figure 5. Comparative (a) Raman Spectra, (b) XRD patterns and (c) TGA curves of GO (control) before and, Zn-GO and Cu-GO after loading of Zn and Cu ions.

After confirming the structure and chemical composition of the prepared Cu-GO and Zn-GO composites, in the last characterization experiment we quantified the amount of Zn and Cu micronutrients loaded on GO sheets using standard methods by the open vessel *aqua regia* extraction method.[59, 60] It was found that 135 mg g^{-1} of Zn and 100 mg g^{-1} of Cu were loaded on the GO sheets. These results are in agreement with the TGA analysis during combustion of the Zn-

GO and Cu-GO composites, showing their Zn and Cu loading around 14 % and 10 %, respectively. Considering that our prepared GO carriers were not optimised in terms of the maximised density of active cites (oxygen groups) it is expected that the observed loading capacity of GO can be further improved if required.

To evaluate the nutrients release of Zn-GO and Cu-GO pellets (i.e. in a granular form comparable to commercial granular fertilizers), a series of experiments were performed to determine their water solubility, dissolution and release rate in a column perfusion method, and their release rate in soil. The water solubility results of Zn-GO and Cu-GO granules compared with $ZnSO_4$ and $CuSO_4$ granules are presented in Figure 6a. Results show that the Zn-GO and Cu-GO granules released only 40 % and 44% of their nutrients compared with 100% of $ZnSO_4$ and $CuSO_4$ granules under the same conditions.

Figure 6b shows the Zn and Cu ions release profile compared with controls obtained by column perfusion method. Again, a significant difference in release rate was observed between Zn-GO and Cu-GO and $ZnSO_4$ and $CuSO_4$ granules. The release for both systems showed a biphasic behaviour consisting of an initial burst release for 5 h, followed by a slow release that was monitored over 72 h. However, during this burst release only ~30 % of Zn and Cu ions were released from GO carriers compared to 75-80% released from $ZnSO_4$ and $CuSO_4$ granules. The rapid initial release of nutrients in first 5 h is likely related to the release of physiosorbed metal salts or loosely adhered metal ions to the surface of the GO sheets. The increasing amount of sulphur (S) in the XPS survey spectra of Cu-GO and Zn-GO (2.02% and 1.69%, respectively) compared to the amount of S in the GO sheets (0.67%) confirms the physical attachment of $ZnSO_4$ and $CuSO_4$ salts during the loading process (Supporting Information, Table S4). In case of $ZnSO_4$ and $CuSO_4$ fertilizers, almost all Zn and Cu was released within 20 h, compared to 50% from GO based granules that showed very slow release rate of ~55 % after 72 h.

The pH of elutes from the column experiment was evaluated for all tested samples to determine the influence of released ions on the pH of solution (Figure 6c). During the burst-phase of the release (first 5 h), the pH of the Zn-GO treatment was initially higher than that for the $ZnSO_4$ granules. Both Zn-GO and $ZnSO_4$ showed a slight increase in the pH of the leachate within the first few h, after which the pH remained constant over time (Figure 6c). The reason for the slight increase of leachate pH during the leaching test from the column for Zn-based fertilizers could be related to proton consumption during dissolution of Zn species from the surface of the fertilizers granules.[61, 62] In contrast, the pH of the initial fractions from the columns with $CuSO_4$ and Cu-GO decreased from 6.5 to 3.6 for $CuSO_4$ and 3.4 for Cu-GO within the first few hours (2 h for $CuSO_4$ and 4 h Cu-GO). However, once the dissolution of the $CuSO_4$ granules was complete, the column elutes tended towards the higher pH values that result from the percolating solution (0.01 mol L^{-1} $CaCl_2$, pH 6.5). For Cu-GO, the pH of elute did not converge to the pH of the calcium chloride ($CaCl_2$) solution because the dissolution process continued and was not

complete. The significant decrease in the eluted solution from the columns with Cu can be explained by the effect of pH on the speciation of Cu. As discussed previously, at higher pH (pH > 6), hydrolysed Cu species are the prominent Cu species. The hydrolysis of Cu ions to soluble $Cu(OH)_2$ produces H^+ ions, which makes the leachate acidic. The pH was lower for the Cu-GO treatment than for the $CuSO_4$ treatment. This may be related to the physiosorbed acid on the GO sheets during the adsorption process of the Cu ions on the GO sheets, which was conducted under acidic conditions (pH=4.5).

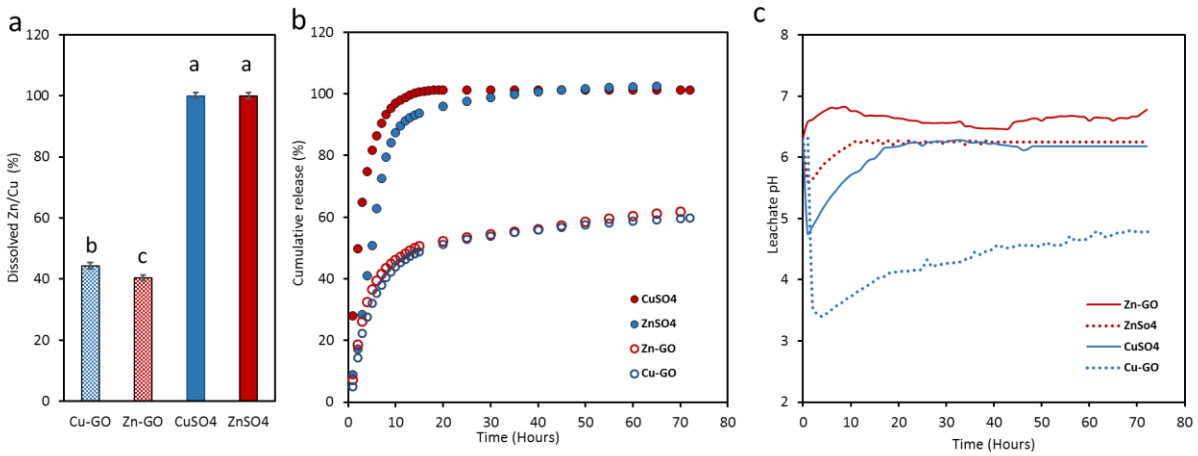

Figure 6. (a) Batch water solubility of Zn and Cu from Zn-GO, Cu-GO, $ZnSO_4$ and $CuSO_4$ fertilizers, (b) kinetic release study of Zn from Zn-GO and $ZnSO_4$, and Cu from Cu-GO and $CuSO_4$ from the columns, and (c) changes in the pH of the elutes from the columns as a function of time. Error bars represents standard error (n=3). Bars with different letters are significantly different at a 5% significance level.

This significant difference in the release pattern of the micronutrients from the GO-based carriers compared to the $ZnSO_4$ and $CuSO_4$ salts is explained by tight coordination of the metal ions and oxygen functional groups on the GO surface.[63] The metal ions can also form a strong complex of Zn^{+2} or Cu^{+2} with two adjacent carboxylate groups or an adjacent phenolic OH group and carboxylate groups at the edges of GO sheets.[63-65] In case of Zn^{+2} and Cu^{+2}, Zn^{+2} is a d^{10} ion and its complexes possess a single ground state; Cu^{+2} is a d^9 ion and its complexes possess a double ground state.[66] The Cu^{+2} tends to bind in a *syn* conformation with oxygen containing functional groups (e.g., carboxylate groups), whereas Zn^{+2} ions are more likely to bind in a direct conformation, while they are sharing two oxygen atom of same carboxylic group (Figure 7a and b).[63, 67] Furthermore, the GO sheets might be bridged by metal ions through the complexation with hydroxyl or carboxyl groups at the edges of GO sheets.[65] Therefore, the release of Zn and Cu will be slower compare to the $ZnSO_4$ and $CuSO_4$ salts due to their strong attachment to GO sheets.

Another mechanism for the slow release of nutrients from GO-based fertilizers is the low accessibility of nutrients in the GO matrix due to the trapping of loaded nutrients between GO sheets. After adding the metal ions to the GO suspension, aggregates form due to the reduction of electrostatic repulsion of Zn and Cu-loaded GO sheets and the Zn and Cu loaded sheets.[32, 64]

It can be seen from SEM images of freeze-dried Zn and Cu loaded GO sheets (Figure 7c), that the GO sheets are folded and create a rod-like structure. They are also wrinkled (Figure 7d) and stacked against each other in the aggregates. The wrinkled and rolled GO sheets stack on top of each other more during the preparation process of Zn-GO or Cu-GO granules (Figures 7e and 7f). Therefore, water molecules have to penetrate through the interconnected channels formed between the rolled or agglomerated GO sheets to release Zn and Cu (Figure 7g), which is a time consuming process.

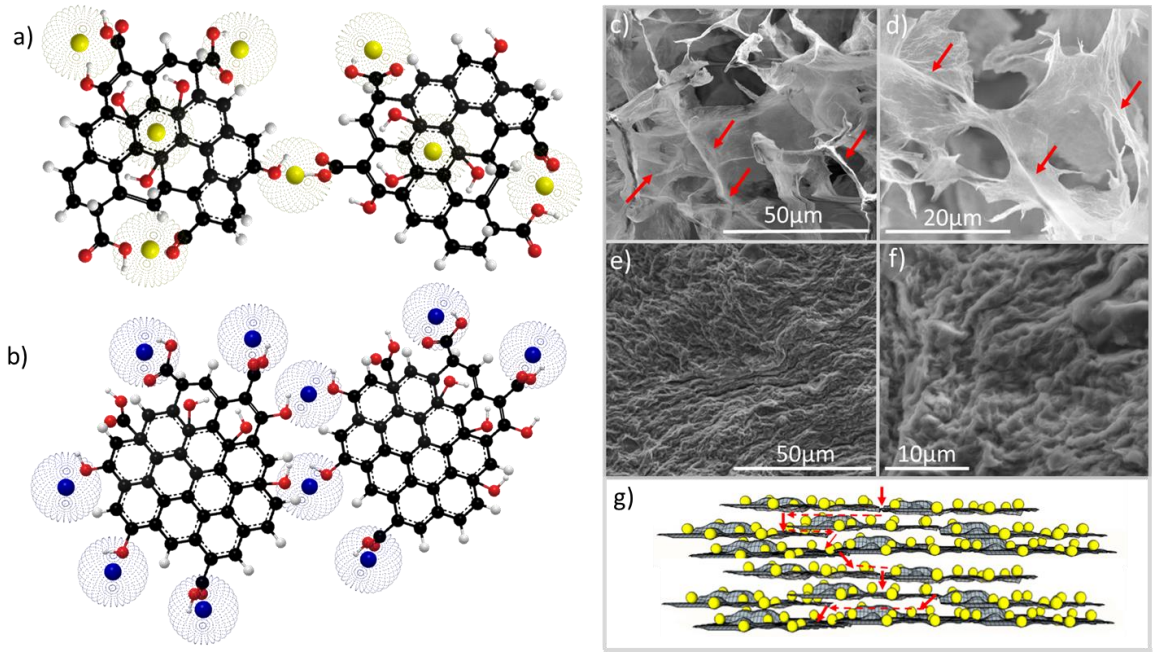

Figure 7. Schematic diagram of GO sheets interactions with (a) Zn^{+2} ions, (b) Cu^{+2} ions, and SEM images of (c) rolled Zn and Cu loaded GO sheets, (d) rolled and wrinkled GO sheets, and (e) low resolution and (f) high resolution SEM images of Cu loaded GO sheets stacked on top of each other, and (g) Schematic of water penetration through the stacked structure of fertilizers granules.

The mechanism of Zn and Cu ions release from Zn-GO and Cu-GO carriers was described and interpreted with using two kinetic models, known as the zero-order and first-order models (Eqs. 1-2).[68, 69]

$$\frac{M_t}{M_\infty} = k.t \quad (1)$$

$$\frac{M_t}{M_\infty} = 1\text{-}\exp^{(-k.t)} \quad (2)$$

where M_t and M_∞ represent the amount of nutrient released at time t and equilibrium, respectively, and k is a solubility rate constant. These two equations have been already used in the prediction of the controlled release of drugs and mineral components of fertilizers.[68, 70, 71] The predicted values calculated by the first-order model for release of nutrient from the starting fertilizers (Zn-GO and Cu-GO) satisfactory fit the experimental data. The correlation coefficients for Zn and Cu solubility rate calculated by the first-order model were 0.92 and 0.95 for Zn-GO and Cu-GO composites, respectively (Supporting Information, Figure S5).

Furthermore, the slope of regression line between observed and predicted values yielded a slope of 0.95 and 0.94, respectively, which shows the strength of using a first-order kinetic model to explain release of nutrient form GO matrix (Supporting Information, Figure S6). Conversely, the zero-order kinetic model did not describe nutrient release well.

Furthermore, the diffusion and transport of released Zn and Cu ions from prepared Zn-GO and Cu-GO granules was examined in soil over 28 days using a visualization method.[72] This technique mimics real conditions in soil and is designed to explore the release, and distribution rate of micronutrients in soil and their potential availability for plants. The visualized Zn and Cu ion distribution for all formulations from day 1 to day 28 is presented in (Supporting Information S7). The visualized Zn and Cu ions distribution zones at 28 days after application of $ZnSO_4$, Zn-GO, $CuSO_4$ and Cu-GO fertilizers in the soil are shown in Figure 8a. The diffusion of Zn and Cu was initially greater when added as $ZnSO_4$ and $CuSO_4$ compared to Zn-GO and Cu-GO ($P<0.05$) (Figure 8b). For all components, the radius of the diffusion zone decreased between day 1 and day 7 which can be explained by continues sorption of Cu and Zn in soil around fertilizer granules. Within a day, diffusion transported Zn and Cu over a volume of soil that had enough adsorption capacity to strongly retain the Zn and Cu and their further movements was slower.[72] Furthermore, lower diffusion of Cu from Cu-based materials compared to Zn diffusion from Zn-based fertilizers was related to the lower mobility of Cu in the soil.[73]

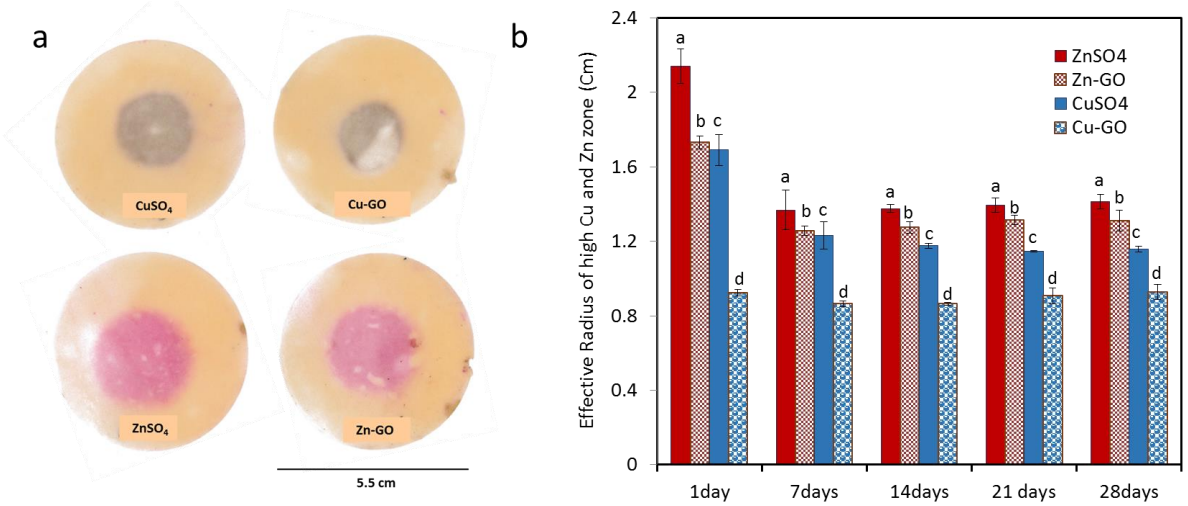

Figure 8. (a) Visualized Zn and Cu diffusion zones in an acid soil (Tumby Bay, Supporting Information Table 1) from $CuSO_4$, Cu-GO, $ZnSO_4$ and Zn-GO fertilizer granules (containing 10 mg of nutrient) added in the centre of a Petri dish filled with the soil and incubated for 28 days, and (b) radius of the high-Zn and high-Cu zone (derived as $\sqrt{A/\pi}$ with A the area of the Zn and Cu diffusion zone) at 1, 7, 14, 21 and 28 days after the addition of Zn-GO, Cu-GO , $ZnSO_4$ and $CuSO_4$ fertilizers. Error bars represents standard error (n=3). Bars with different letters are significantly different (at a 5% significance level) at a given time point.

Results of the chemical analysis of the soil are presented in Table 3. Concentrations of Zn and Cu in the diffusion zones in soil matched the visualization results. In the case of $ZnSO_4$ and

Zn-GO granules, similar amounts of Zn were recovered at >9 mm from the granules, 30% and 28%, respectively. In soil with $CuSO_4$ granules, 31.5% of the fertilizer Cu was recovered at >9 mm while in soil with Cu-GO granules 19% of the fertilizer Cu was recovered in this zone.

Table 3. Chemical analysis results on soil concentrically sampled around the fertilizer application sites at 28 days after addition of Zn and Cu fertilizers (at 10 mg Zn; $ZnSO_4$, Zn-GO and 10 mg Cu; $CuSO_4$ and Cu-GO). pH and solution concentrations of Zn and Cu in a 1 mM $CaCl_2$ extract from different soil sections and the percentage of added Zn and Cu recovered at <9mm from the granules were measured (standard error of 3 replicates between brackets).

Fertilizer	**pH**		**Zn or Cu solution concentration (µg/L)**		**% of added metal (Zn or Cu)**	
	<9mm	**>9mm**	**<9mm**	**>9mm**	**at<9mm**	**at>9mm**
$ZnSO_4$	6.55(0.02)	6.42(0.08)	2067(67.5)	289(23.2)	70(0.00)	30.0(0.00)
Zn-GO	6.62(0.07)	6.33(0.02)	4199(69.8)	570(46.5)	71(0.06)	28.0(0.00)
$CuSO_4$	6.08(0.06)	6.40(0.03)	2209(85.1)	331(19.4)	68(0.02)	31.5(0.00)
Cu-GO	6.20(0.05)	6.40(0.05)	2395(179)	148(23.7)	82(0.01)	19.0(0.01)

Finally, the efficiency of Zn-GO and Cu-GO fertilizers for improving yield and Zn or Cu content of durum wheat (*Triticum durum cv.* Yallaroi) was studied. The grain dry mass was higher when the soil was fertilized with Zn-GO compared to the soil fertilized with $ZnSO_4$ granules ($P<0.05$) (Figure 9a). However, there was no difference in plant dry mass for soil treated with Cu-GO and $CuSO_4$ fertilizers ($P>0.05$)(Figure 9b), because this soil was not Cu-responsive, as evident from similar yield for the control (no Cu) and the Cu-amended treatments. Regarding nutrient uptake, plants treated with the Zn-GO fertilizer showed significantly higher nutrient uptake than those treated with Zn salts and the control ($P<0.05$) (Figure 9c). The Cu uptake was slightly higher for the Cu-GO fertilizer than for the Cu salt and control treatments, but this difference was not significant (Figure 9d). The lower uptake in the treatments with Zn salt is likely related to fixation of Zn in this calcareous soil, e.g. due to irreversible adsorption on carbonates or precipitation as Zn hydroxides or carbonate. Compared with Zn and Cu salts, GO is able to form stronger complex with Zn or Cu and, and thus Zn-GO and Cu-GO may have less interaction with the soil components, keeping these micronutrients in more available forms to be taken up by the plants.[74]

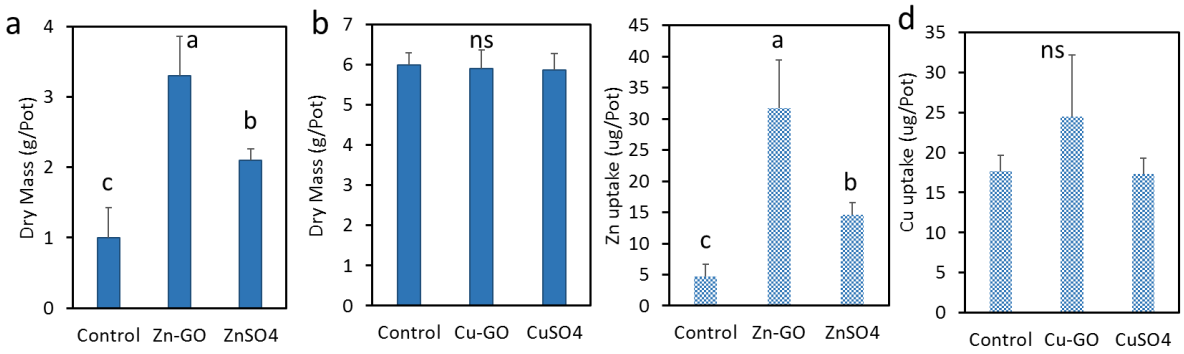

Figure 9. (a) Effect of different Zn, (b) different Cu formulations on grain yield (dry mass) of wheat and (c, d) effect of different Zn and Cu formulations on nutrient uptake by plant. Error bars represents standard error (n=3). Bars with different letters are significantly different at a 5% significance level and bars with ns are not significantly different.

To the best of our knowledge, this is the first report on the agronomic performance of novel GO-based slow-release micronutrient fertilizers compared to traditional, fully soluble salts. This study clearly shows promise for the developed GO-based nutrient carriers with a slow-release pattern as new fertilizer materials.

CONCLUSION

In this study, we have demonstrated the use of GO sheets as a new carrier for nutrients, resulting in a slow release and sustained delivery of micronutrients such as Zn and Cu. The micronutrient fertilizers (Zn-GO and Cu-GO) prepared in the form of solid pellets showed a high nutrient loading capacity (more than 10%) which is related to the high surface area of GO and high density of oxygen binding sites on the surface and edge of GO, responsible for binding the micronutrients ions. The GO-based carrier had a biphasic nutrient release characteristic with an ability to supply micronutrients in both fast-release (ca 40% for 5 h) and slow sustained release. This release pattern is highly desirable and advantageous for the crops where seedling establishment needs high nutrient loadings, and at later stages of crops growth a slower and sustained release of micronutrients is needed. The significant loading and desirable release performances of GO-based carriers make them favourable material for loading of any nutrient (macro, micro and their combinations) and therefore they could be used as generic carriers for creating of new generation of advanced SRFs. Given that the price of commercially produced GO will most likely significantly decrease in the near future, there is strong prospective that industrial-scale production of these high performing graphene-based fertilisers will become commercially feasible over time.

Supporting Information

Supporting information provides supplementary texts, figures and tables which includes: **Experimental section** including: graphene oxide (GO) preparation, Batch adsorption and pH

experiments, Cu and Zn loading on graphene oxide sheets , Dissolution kinetics study of Zn-GO and Cu-GO fertilizers using column perfusion, Zinc and copper diffusion visualization method Measuring soil pH and total Zn and Cu in the soil, Plant study and, Characterizations and statistical analysis, **Table S1** with selected physical and chemical properties of the soil used in soil diffusion study, **Table S2** with selected physical and chemical properties of the soil used in plant study, **Table S3** with concentration of basal nutrient solution applied to each pot, Fourier transform infrared spectroscopy (FTIR and high resolution XPS peaks (**Figure S1**), Thermodynamic speciation of Zn and Cu ions (**Figure S2**), kinetic models of pseudo-first-order and pseudo-second-order (**Figure S3**), **Table S4** Kinetic parameters of the pseudo-first order and pseudo-second order equations for Zn^{+2} and Cu^{+2} sorption on GO, **Table S5**, Percent elemental concentration for GO, Zn-GO and Cu-GO composites from XPS survey scans XPS characteristics of GO sheets, b) Zn-GO and c) Cu-GO (**Figure S4**), Mathematical release models of a) Zero-order and b) First-order models of Zn-GO, and c) Zero-order and d) First-order model of Cu-GO (**Figure S5**). The cumulative release of nutrients from slow released a) Zn-GO and b) Cu-GO fertilizers (**Figure S6**) and Visualized copper diffusion from a) $CuSO_4$ and b) Cu-GO, and Visualized zinc diffusion from a) ZnSO4 and b) Zn-GO at 1, 7, 14, 21 and 28 days of incubation (**Figure S7**).

ACKNOWLEDGEMENTS

The authors thank the support of the Australian Research Council (ARC) funding ARC DP 150101760 and ARC IH 150100003 (Graphene Enabled Industry Transformation) for financial support to this work. The support from The University of Adelaide and the Schools of Chemical Engineering and Agriculture, Food and Wine is acknowledged.

References

1. Zhang, M.; Gao, B.; Chen, J.; Li, Y.; Creamer, A. E.; Chen, H. Slow-release fertilizer encapsulated by graphene oxide films. *Chemical Engineering Journal* 2014, 255, 107-113.
2. McBeath, T. M.; , M. J. M. Efficacy of zinc oxide as fertilizers. *Plant Soil* 2014, 374, 843-855.
3. Zhao, A.-q.; Tian, X.-h.; Chen, Y.-l.; Li, S. Application of ZnSO4 or Zn-EDTA fertilizer to a calcareous soil: Zn diffusion in soil and its uptake by wheat plants. *Journal of the Science of Food and Agriculture* 2015, n/a-n/a.
4. Zhu, Q.; Zhang, M.; Ma, Q. Copper-based foliar fertilizer and controlled release urea improved soil chemical properties, plant growth and yield of tomato. *Scientia Horticulturae* 2012, 143, 109-114.
5. Li, P.; Li, L.; Du, Y.; Hampton, M. A.; Nguyen, A. V.; Huang, L.; Rudolph, V.; Xu, Z. P. Potential foliar fertilizers with copper and zinc dual micronutrients in nanocrystal suspension. *Journal of Nanoparticle Research* 2014, 16, 1-11.
6. Ray, S. K.; Varadachari, C.; Ghosh, K. Novel Slow-Releasing Micronutrient Fertilizers. 2. Copper Compounds. *Journal of Agricultural and Food Chemistry* 1997, 45, 1447-1453.

7. Bandyopadhyay, S.; Ghosh, K.; Varadachari, C. Multimicronutrient Slow-Release Fertilizer of Zinc, Iron, Manganese, and Copper. *International Journal of Chemical Engineering* 2014, 2014, 7.
8. Rico, M. I.; Alvarez, J. M.; Vallejo, A. Preparation of Fertilizers with Rosin and Tricalcium Phosphate Coated Zinc Chelates. Laboratory Characterization. *Journal of Agricultural and Food Chemistry* 1995, 43, 2758-2761.
9. Jin, S.; Yue, G.; Feng, L.; Han, Y.; Yu, X.; Zhang, Z. Preparation and Properties of a Coated Slow-Release and Water-Retention Biuret Phosphoramide Fertilizer with Superabsorbent. *Journal of Agricultural and Food Chemistry* 2011, 59, 322-327.
10. Sanjay K. ray, C. V. a. K. G. Novel Slow-Releasing Micronutrient Fertilizers. 1. Zinc compounds. *Indian. Eng. Chem. Res* 1993, 32, 1218-1227.
11. Krems-Chemie. Complete fertilizers containing trace elements. 1975.
12. Volfkovich, S. Polymeric fertilizers. *J. Appl. Chem.(USSR)* 1972, 45, 2479-2487.
13. Ray, S. K.; Varadachari, C.; Ghosh, K. Novel slow-releasing micronutrient fertilizers. 1. Zinc compounds. *Industrial & Engineering Chemistry Research* 1993, 32, 1218-1227.
14. W, L. J.; A, R. G.; L, V. H. Methods for preparing mixed cation polyphosphates. Google Patents: 1971.
15. Bandyopadhyay, S.; Bhattacharya, I.; Ghosh, K.; Varadachari, C. New slow-releasing molybdenum fertilizer. *Journal of agricultural and food chemistry* 2008, 56, 1343-1349.
16. Geim, A. K.; Novoselov, K. S. The rise of graphene. *Nature materials* 2007, 6, 183-191.
17. Allen, M. J.; Tung, V. C.; Kaner, R. B. Honeycomb carbon: a review of graphene. *Chemical reviews* 2009, 110, 132-145.
18. Eda, G.; Chhowalla, M. Chemically derived graphene oxide: towards large-area thin-film electronics and optoelectronics. *Advanced Materials* 2010, 22, 2392-2415.
19. Wang, K.; Ruan, J.; Song, H.; Zhang, J.; Wo, Y.; Guo, S.; Cui, D. Biocompatibility of graphene oxide. *Nanoscale Res Lett* 2011, 6, 1-8.
20. Perreault, F.; Fonseca de Faria, A.; Elimelech, M. Environmental applications of graphene-based nanomaterials. *Chemical Society Reviews* 2015, 44, 5861-5896.
21. Dreyer, D. R.; Park, S.; Bielawski, C. W.; Ruoff, R. S. The chemistry of graphene oxide. *Chemical Society Reviews* 2010, 39, 228-240.
22. Jin, L.; Yang, K.; Yao, K.; Zhang, S.; Tao, H.; Lee, S.-T.; Liu, Z.; Peng, R. Functionalized Graphene Oxide in Enzyme Engineering: A Selective Modulator for Enzyme Activity and Thermostability. *ACS Nano* 2012, 6, 4864-4875.
23. Liu, Z.; Robinson, J. T.; Sun, X.; Dai, H. PEGylated Nano-Graphene Oxide for Delivery of Water Insoluble Cancer Drugs. *Journal of the American Chemical Society* 2008, 130, 10876-10877.
24. Liu, J.; Cui, L.; Losic, D. Graphene and graphene oxide as new nanocarriers for drug delivery applications. *Acta Biomaterialia* 2013, 9, 9243-9257.
25. Pan, Y.; Sahoo, N. G.; Li, L. The application of graphene oxide in drug delivery. *Expert Opinion on Drug Delivery* 2012, 9, 1365-1376.
26. Shen, H.; Zhang, L.; Liu, M.; Zhang, Z. Biomedical Applications of Graphene. *Theranostics* 2012, 2, 283-294.
27. Liu, Z.; Robinson, J. T.; Sun, X.; Dai, H. PEGylated Nanographene Oxide for Delivery of Water-Insoluble Cancer Drugs. *Journal of the American Chemical Society* 2008, 130, 10876-10877.
28. Ocsoy, I.; Paret, M. L.; Ocsoy, M. A.; Kunwar, S.; Chen, T.; You, M.; Tan, W. Nanotechnology in Plant Disease Management: DNA-Directed Silver Nanoparticles on Graphene Oxide as an Antibacterial against Xanthomonas perforans. *ACS Nano* 2013, 7, 8972-8980.
29. Zhao, J.; Wang, Z.; White, J. C.; Xing, B. Graphene in the Aquatic Environment: Adsorption, Dispersion, Toxicity and Transformation. *Environmental Science & Technology* 2014, 48, 9995-10009.
30. Zhao, G.; Li, J.; Ren, X.; Chen, C.; Wang, X. Few-Layered Graphene Oxide Nanosheets As Superior Sorbents for Heavy Metal Ion Pollution Management. *Environmental Science & Technology* 2011, 45, 10454-10462.

31. Sitko, R.; Turek, E.; Zawisza, B.; Malicka, E.; Talik, E.; Heimann, J.; Gagor, A.; Feist, B.; Wrzalik, R. Adsorption of divalent metal ions from aqueous solutions using graphene oxide. *Dalton Transactions* 2013, 42, 5682-5689.
32. Yang, S.-T.; Chang, Y.; Wang, H.; Liu, G.; Chen, S.; Wang, Y.; Liu, Y.; Cao, A. Folding/aggregation of graphene oxide and its application in Cu2+ removal. *Journal of Colloid and Interface Science* 2010, 351, 122-127.
33. Zhao, G.; Ren, X.; Gao, X.; Tan, X.; Li, J.; Chen, C.; Huang, Y.; Wang, X. Removal of Pb(ii) ions from aqueous solutions on few-layered graphene oxide nanosheets. *Dalton Transactions* 2011, 40, 10945-10952.
34. Kabiri, S.; Tran, D. N. H.; Azari, S.; Losic, D. Graphene-Diatom Silica Aerogels for Efficient Removal of Mercury Ions from Water. *ACS Applied Materials & Interfaces* 2015, 7, 11815-11823.
35. Madadrang, C. J.; Kim, H. Y.; Gao, G.; Wang, N.; Zhu, J.; Feng, H.; Gorring, M.; Kasner, M. L.; Hou, S. Adsorption Behavior of EDTA-Graphene Oxide for Pb (II) Removal. *ACS Applied Materials & Interfaces* 2012, 4, 1186-1193.
36. Deng, X.; Lü, L.; Li, H.; Luo, F. The adsorption properties of Pb(II) and Cd(II) on functionalized graphene prepared by electrolysis method. *Journal of Hazardous Materials* 2010, 183, 923-930.
37. Zhang, X.; Yin, J.; Peng, C.; Hu, W.; Zhu, Z.; Li, W.; Fan, C.; Huang, Q. Distribution and biocompatibility studies of graphene oxide in mice after intravenous administration. *Carbon* 2011, 49, 986-995.
38. Chang, Y.; Yang, S.-T.; Liu, J.-H.; Dong, E.; Wang, Y.; Cao, A.; Liu, Y.; Wang, H. In vitro toxicity evaluation of graphene oxide on A549 cells. *Toxicology Letters* 2011, 200, 201-210.
39. Ryoo, S.-R.; Kim, Y.-K.; Kim, M.-H.; Min, D.-H. Behaviors of NIH-3T3 Fibroblasts on Graphene/Carbon Nanotubes: Proliferation, Focal Adhesion, and Gene Transfection Studies. *ACS Nano* 2010, 4, 6587-6598.
40. Strayer, A.; Ocsoy, I.; Tan, W.; Jones, J. B.; Paret, M. L. Low Concentrations of a Silver-Based Nanocomposite to Manage Bacterial Spot of Tomato in the Greenhouse. *Plant Disease* 2015, 100, 1460-1465.
41. Akhavan, O.; Ghaderi, E. Toxicity of Graphene and Graphene Oxide Nanowalls Against Bacteria. *ACS Nano* 2010, 4, 5731-5736.
42. Xu, W.-P.; Zhang, L.-C.; Li, J.-P.; Lu, Y.; Li, H.-H.; Ma, Y.-N.; Wang, W.-D.; Yu, S.-H. Facile synthesis of silver@graphene oxide nanocomposites and their enhanced antibacterial properties. *Journal of Materials Chemistry* 2011, 21, 4593-4597.
43. Akhavan, O.; Ghaderi, E. Escherichia coli bacteria reduce graphene oxide to bactericidal graphene in a self-limiting manner. *Carbon* 2012, 50, 1853-1860.
44. Bianco, A.; Kostarelos, K.; Prato, M. Applications of carbon nanotubes in drug delivery. *Current Opinion in Chemical Biology* 2005, 9, 674-679.
45. Lalwani, G.; Xing, W.; Sitharaman, B. Enzymatic Degradation of Oxidized and Reduced Graphene Nanoribbons by Lignin Peroxidase. *Journal of materials chemistry. B, Materials for biology and medicine* 2014, 2, 6354-6362.
46. Kotchey, G. P.; Allen, B. L.; Vedala, H.; Yanamala, N.; Kapralov, A. A.; Tyurina, Y. Y.; Klein-Seetharaman, J.; Kagan, V. E.; Star, A. The Enzymatic Oxidation of Graphene Oxide. *ACS Nano* 2011, 5, 2098-2108.
47. Allen, B. L.; Kichambare, P. D.; Gou, P.; Vlasova, I. I.; Kapralov, A. A.; Konduru, N.; Kagan, V. E.; Star, A. Biodegradation of Single-Walled Carbon Nanotubes through Enzymatic Catalysis. *Nano Letters* 2008, 8, 3899-3903.
48. Fang, R.; Liang, Y.; Ge, X.; Du, M.; Li, S.; Li, T.; Li, Z. Preparation and photocatalytic degradation activity of TiO2/rGO/polymer composites. *Colloid and Polymer Science* 2015, 293, 1151-1157.
49. Marcano, D. C.; Kosynkin, D. V.; Berlin, J. M.; Sinitskii, A.; Sun, Z.; Slesarev, A.; Alemany, L. B.; Lu, W.; Tour, J. M. Improved Synthesis of Graphene Oxide. *ACS Nano* 2010, 4, 4806-4814.

50. Sydlik, S. A.; Jhunjhunwala, S.; Webber, M. J.; Anderson, D. G.; Langer, R. In Vivo Compatibility of Graphene Oxide with Differing Oxidation States. *ACS Nano* 2015, 9, 3866-3874.
51. Trent William Jay Albrecht*, J. A.-M. a. D. F. Effect of pH, Concentration and Temperature on Copper and Zinc Hydroxide Formation/Precipitation in Solution In *Chemeca*, Australia, 2011.
52. Zhao, G.; Wen, T.; Yang, X.; Yang, S.; Liao, J.; Hu, J.; Shao, D.; Wang, X. Preconcentration of U(vi) ions on few-layered graphene oxide nanosheets from aqueous solutions. *Dalton Transactions* 2012, 41, 6182-6188.
53. Lim, S.-F.; Lee, A. Kinetic study on removal of heavy metal ions from aqueous solution by using soil. *Environmental Science and Pollution Research* 2015, 22, 10144-10158.
54. Li, R.; Liang, J.; Hou, Y.; Chu, Q. Enhanced corrosion performance of Zn coating by incorporating graphene oxide electrodeposited from deep eutectic solvent. *RSC Advances* 2015, 5, 60698-60707.
55. Marimuthu, M.; Veerapandian, M.; Ramasundaram, S.; Hong, S. W.; Sudhagar, P.; Nagarajan, S.; Raman, V.; Ito, E.; Kim, S.; Yun, K.; Kang, Y. S. Sodium functionalized graphene oxide coated titanium plates for improved corrosion resistance and cell viability. *Applied Surface Science* 2014, 293, 124-131.
56. Larciprete, R.; Lacovig, P.; Gardonio, S.; Baraldi, A.; Lizzit, S. Atomic oxygen on graphite: Chemical characterization and thermal reduction. *Journal of Physical Chemistry C* 2012, 116, 9900-9908.
57. Rupp, J. L. M.; Infortuna, A.; Gauckler, L. J. Microstrain and self-limited grain growth in nanocrystalline ceria ceramics. *Acta Materialia* 2006, 54, 1721-1730.
58. Stankovich, S.; Dikin, D. A.; Piner, R. D.; Kohlhaas, K. A.; Kleinhammes, A.; Jia, Y.; Wu, Y.; Nguyen, S. T.; Ruoff, R. S. Synthesis of graphene-based nanosheets via chemical reduction of exfoliated graphite oxide. *Carbon* 2007, 45, 1558-1565.
59. Milani, N.; McLaughlin, M. J.; Stacey, S. P.; Kirby, J. K.; Hettiarachchi, G. M.; Beak, D. G.; Cornelis, G. Dissolution Kinetics of Macronutrient Fertilizers Coated with Manufactured Zinc Oxide Nanoparticles. *Journal of Agricultural and Food Chemistry* 2012, 60, 3991-3998.
60. Tandy, S.; Bossart, K.; Mueller, R.; Ritschel, J.; Hauser, L.; Schulin, R.; Nowack, B. Extraction of Heavy Metals from Soils Using Biodegradable Chelating Agents. *Environmental Science & Technology* 2004, 38, 937-944.
61. Degen, A.; Kosec, M. Effect of pH and impurities on the surface charge of zinc oxide in aqueous solution. *Journal of the European Ceramic Society* 2000, 20, 667-673.
62. Bian, S.-W.; Mudunkotuwa, I. A.; Rupasinghe, T.; Grassian, V. H. Aggregation and Dissolution of 4 nm ZnO Nanoparticles in Aqueous Environments: Influence of pH, Ionic Strength, Size, and Adsorption of Humic Acid. *Langmuir* 2011, 27, 6059-6068.
63. Sun, P.; Zhu, M.; Wang, K.; Zhong, M.; Wei, J.; Wu, D.; Xu, Z.; Zhu, H. Selective Ion Penetration of Graphene Oxide Membranes. *ACS Nano* 2013, 7, 428-437.
64. Peng, W.; Li, H.; Liu, Y.; Song, S. Comparison of Pb(II) adsorption onto graphene oxide prepared from natural graphites: Diagramming the Pb(II) adsorption sites. *Applied Surface Science* 2016, 364, 620-627.
65. Peng, W.; Li, H.; Liu, Y.; Song, S. A review on heavy metal ions adsorption from water by graphene oxide and its composites. *Journal of Molecular Liquids* 2017, 230, 496-504.
66. Rulíšek, L.; Havlas, Z. Theoretical Studies of Metal Ion Selectivity. 1. DFT Calculations of Interaction Energies of Amino Acid Side Chains with Selected Transition Metal Ions (Co2+, Ni2+, Cu2+, Zn2+, Cd2+, and Hg2+). *Journal of the American Chemical Society* 2000, 122, 10428-10439.
67. Carrell, C. J.; Carrell, H. L.; Erlebacher, J.; Glusker, J. P. Structural aspects of metal ion carboxylate interactions. *Journal of the American Chemical Society* 1988, 110, 8651-8656.
68. Szepes, A.; Ulrich, J.; Farkas, Z.; Kovács, J.; Szabó-Révész, P. Freeze-casting technique in the development of solid drug delivery systems. *Chemical Engineering and Processing: Process Intensification* 2007, 46, 230-238.

69. Costa, P.; Sousa Lobo, J. M. Modeling and comparison of dissolution profiles. *European Journal of Pharmaceutical Sciences* 2001, 13, 123-133.
70. T. Jamnongkan, S. K. Controlled-Release Fertilizer Based on Chitosan Hydrogel:

Phosphorus Release Kinetics. *SCIENCE JOURNAL*

Ubonratchathani University 2010, 1, 43-50.
71. Yang, Y.-C.; Zhang, M.; Zheng, L.; Cheng, D.-D.; Liu, M.; Geng, Y.-Q. Controlled Release Urea Improved Nitrogen Use Efficiency, Yield, and Quality of Wheat All rights reserved. No part of this periodical may be reproduced or transmitted in any form or by any means, electronic or mechanical, including photocopying, recording, or any information storage and retrieval system, without permission in writing from the publisher. *Agronomy Journal* 2011, 103, 479-485.
72. Degryse, F.; Baird, R.; McLaughlin, M. Diffusion and solubility control of fertilizer-applied zinc: chemical assessment and visualization. *Plant and Soil* 2015, 386, 195-204.
73. D.Harter, R. *Micronutrient Adsorption-Desorption Reactions in Soils*. SSSA Inc, Madison: 1991.
74. Zhao, A.-q.; Tian, X.-h.; Chen, Y.-l.; Li, S. Application of ZnSO4 or Zn-EDTA fertilizer to a calcareous soil: Zn diffusion in soil and its uptake by wheat plants. *Journal of the Science of Food and Agriculture* 2016, 96, 1484-1491.